Data-driven method for optimized supply temperatures in residential buildings

Pothof, I.; Vreeken, D.; Meerkerk, M. van

DOI
10.1016/j.energy.2023.129183

Publication date
2023

Document Version
Final published version

Published in
Energy

Citation (APA)
Pothof, I., Vreeken, D., & Meerkerk, M. V. (2023). Data-driven method for optimized supply temperatures in residential buildings. *Energy*, *284*, Article 129183. https://doi.org/10.1016/j.energy.2023.129183

Energy 284 (2023) 129183

Contents lists available at ScienceDirect

Energy

journal homepage: www.elsevier.com/locate/energy

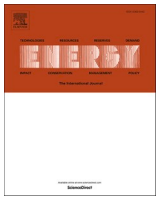

Data-driven method for optimized supply temperatures in residential buildings

I. Pothof [a,b,*], D. Vreeken [a], M. van Meerkerk [a]

[a] Deltares, Delft, Netherlands
[b] Delft University of Technology, Department Water Management, Sustainable District Heating Cooling, Delft, Netherlands

ARTICLE INFO

Handling Editor: Dr X Zhao

Keywords:
Radiator
Supply temperature
Design condition
Measurements

ABSTRACT

The energy required for space heating amounts to approximately 68% of the total energy demand of existing buildings in Europe. The heat requirement of a building, and thus its carbon emission, can be lowered by optimizing the supply and return temperature of the heating system. A lower supply temperature enables a wider variety of transition pathways towards sustainable heating with reduced carbon emissions. However, the minimum supply temperature that guarantees acceptable indoor temperatures in existing dwellings during design weather conditions is still unknown. In this study, we determine the minimum supply temperature by fitting a 2 R–2C model to hourly measurement data. The measurement data is obtained from a representative set of 220 existing gas-fired dwellings in the Netherlands. The heating system of each dwelling was equipped with a pulse flowmeter and temperature sensors on both the supply and return side. Additionally, data was collected from the thermostat in the main living room and the gas boiler. The data was supplemented with weather data from a nearby weather station. The data-driven model shows that the minimum supply temperature can be lower than 55 °C for 60% of the dwellings during design weather conditions (i.e., −10 °C in the Netherlands). Moreover, the minimum supply temperature is poorly correlated with general building properties, such as the building typology, construction period or specific annual space heating demand (kWh/(m^{2}yr)). On the contrary, the ratio between the required and installed heat output of the radiators in the heating system is a promising parameter to predict the minimum design supply temperature of an individual dwelling that guarantees an acceptable indoor temperature during design weather conditions.

1. Introduction

1.1. Background

The space heating demand of residential buildings amounts to 68% of their total energy consumption [1]. The heat demand of residential buildings is often supplied by fossil fuels, which results in heat related carbon emission. The carbon emissions of buildings should be reduced to meet climate policy goals of 2030 [2]. The fossil-based heat supply to residential buildings is characterized by a high supply temperature and corresponding heating power, providing a high level of thermal comfort. Fossil-free heating solutions for individual dwellings and neighborhoods benefit from low supply temperatures for space heating. Therefore, it would be interesting to understand to which level the supply temperature for space heating can be reduced in existing dwellings without any renovation measure.

1.2. Previous work low-temperature heating

Lower supply temperatures have multiple benefits. First, it improves the efficiency of solar collectors and air-source or ground-source heat pumps. Thereby, unlocking the potential of sustainable heat sources such as thermal energy from surface water, wastewater and datacenters and storage in the subsurface. In addition, the increased efficiency of heat supply systems results in lower investment (i.e., lower capacity of heat pump) and operational costs (i.e., less electricity consumption). A lower supply temperature of the heating system might also reduce the energy consumption of buildings [3]. Finally, lower supply temperatures reduce the thermal stresses and distribution heat losses of district heating systems. This results in a reduction of the cost of ownership of the grid.

In recent years, low-temperature (LT)-heating systems have gained attention for their potential to reduce energy consumption, lower operating costs, and decrease greenhouse gas emissions in existing

* Corresponding author. Deltares, Delft, Netherlands.
E-mail address: ivo.pothof@deltares.nl (I. Pothof).

https://doi.org/10.1016/j.energy.2023.129183
Received 25 January 2023; Received in revised form 16 August 2023; Accepted 22 September 2023
Available online 28 September 2023

Nomenclature

Symbol	*Description*
T_s	Measured supply temperature at the gas boiler [°C]
T_r	Measured return temperature at the gas boiler [°C]
T_i	Measured/modelled Indoor temperature at the thermostat in the living room [°C]
T_e	Modelled building envelope temperature [°C]
T_a	Measured ambient temperature at the nearest weather station [°C]
Q_h	Measured/Modelled heat output from heating system [W]
Q_s	Measured solar influx [W/m^2]
A_w	Model parameter for effective window area for solar influx [m^2]
R_{ie}	Model parameter for thermal resistance between indoor space and building envelope [°C/W]
R_{ea}	Model parameter for thermal resistance between building envelope and ambient conditions [°C/W]
C_i	Model parameter for thermal storage in building interior [Wh/°C]
C_e	Model parameter for thermal storage in building envelope [Wh/°C]
Q_d	Design heat output into the building [W]
Q_a	Available, installed heat output in the building [W]
ΔT_{sys}	Differential temperature between gas boiler supply and return temperature ($T_s - T_r$) [°C]
ΔT_{LMTD}	Logarithmic mean temperature difference, based on T_s, T_r and T_i [°C]; defined in section 2
E_s	Annual specific heat demand [kWh/(m^{2}yr)]

Abbreviation	*Explanation*
DHW	Domestic hot water
SH	Space heating
LTDH	Low-temperature District Heating

buildings [4]. Numerical work indicates that low-temperature (district) heating is feasible most of the year with minor building renovations [5–7]. These studies recommend at least minor building improvements, such as double-glazed windows or cavity wall insulation, before LT-heating is feasible. Dynamic building simulations are used to estimate the required supply temperatures [8]. However, such modelling approaches require many assumptions on the actual values of the thermal resistances of the building envelope and windows, Also, infiltration and ventilation losses must be estimated, and occupant behavior causes significant uncertainties in heat demand. Finally, the use of dynamic building simulations is time-consuming for a large-scale experiment with a few hundred dwellings. On the other hand, the heat demand in existing dwellings can be measured directly, such that key properties of the building, radiator system and occupant behavior are captured.

Limited experimental data exists on the actual performance of LT-heating systems in existing buildings, creating a research gap that needs to be addressed. In 2017, Jangsten et al. conducted an experimental study to measure the supply and return temperatures of existing heating systems [9]. The study found that at design conditions of −16 °C in Gothenburg, the average supply temperature was 65 °C. In Denmark, a small-scale experimental study by D. S. Østergaard & Svendsen [10] showed that supply temperatures lower than 55 °C were possible for most of the year in residential buildings. More recently, Benakopoulos, Tunzi et al. [11] developed a strategy for low-temperature operation of radiator systems in a multi-family building. Their study combined the concept of heating degree days and the radiator coefficient to determine the minimum required supply temperature at different outdoor temperatures. The study found that well-controlled heating systems in existing buildings have good potential for LT-operation.

The minimum required supply temperature at design conditions is often not addressed [10]. The minimum required supply temperature of a residential heating system depends on the available radiator capacity [11]. The radiators in buildings are designed to accommodate a high level of thermal comfort. Consequently, most heating systems have oversized radiators at supply and return temperatures of respectively 70 and 40 °C [4,9,12].

There are several reasons for the oversized radiators in existing heating systems. First, advanced computer-aided design methods were not widely available until the late 1980s [13]. Second, the insulation of building envelopes has improved over the years with for example insulation of wall-cavities, floors, roofs and double-glazed windows. Third, climate change reduces the heat demand of buildings. For example, the number of heating degree days in the Netherlands has reduced by 20% over the past 5 decades [14]. Finally, design requirements and the assumption of intermittent operation (i.e., night setback) require oversized radiators [13]. The oversizing factor describes the ratio between available and required radiator output power. A radiator oversizing factor of 30% combined with minor building improvements could already reduce the supply temperature to 50 °C while occasionally requiring supply temperatures of 60 °C [15].

We conclude from the state of the art that many studies recommend building renovations prior to LT-operation. Most of the existing studies conclude that LT-operation is feasible most of the year, but the previous studies are not explicit about the feasibility of LT-heating during design conditions. The oversizing of radiators is identified as an important parameter for LT-readiness. However, it is important to note that the experimental studies are limited in the number of involved buildings and building typologies, which compromises their implications on the LT-readiness of the national building stock. Additionally, the lack of direct measurements of mass or volume flow to the heating system may limit the broader applicability of the findings.

1.3. Scope of study

The key question addressed in this study is to determine the minimum required supply temperature for space heating during design conditions in the Dutch residential buildings, heated with gas boilers, without adopting any renovation measure. A second question is which fraction of the Dutch building stock is suitable for LT-heating. Furthermore, we try to predict the LT-readiness of Dutch dwellings based on

publicly available parameters or straightforward metrics, such as building typology and specific heat demand. These research questions have been addressed with an experimental investigation, conducted between December 2020 and March 2022. We have developed the experimental set-up and a data-driven model to derive the minimum required supply temperature during design conditions. The minimum supply temperature is determined with a grey-box model with experimental data that includes measurements of the volume flow rate, and the supply and return temperatures of the heating system.

1.4. Novelty

This study includes three novel elements. First, the combined measurement of supply and return temperature and flow rates to individual heating systems. Secondly, this monitoring system enables a novel fully data-driven approach to determine the minimum required supply temperature during design conditions. As a consequence, we do not need assumptions on radiator coefficients, mass flow rates or return temperatures. The third novelty is the fairly large sample size of more than 200 dwellings, which gives a first indication of the LT-readiness of the Dutch gas-heated building stock.

The paper is organized as follows. The experimental set-up and equipment are introduced in section 2. This section also introduces the representative sample of existing buildings in the Netherlands and details the data-driven method to determine the minimum supply temperature. Section 3 presents the results on the model calibration, the minimum supply temperatures and proposes a LT-ready metric for existing dwellings. In section 4, the measurement and model results will be discussed. Finally, the last section presents the main findings and provides recommendations for future research.

2. Materials and methods

In this section, we detail the sample of existing buildings in the Netherlands. Thereafter, the measurement equipment is described. Finally, the data-driven method is detailed.

2.1. Representative sample

A representative sample of existing buildings in the Netherlands was selected with support by installation company Feenstra B·V. In the Netherlands, buildings are divided in subsets based on building typology and construction periods. Four building types are identified, namely: apartments, terraced dwellings, corner dwellings, and detached dwellings [16]. In this study, the sample of existing building is divided in three construction periods, namely: before 1974, 1974–1991, and after 1991. Buildings before 1974, in general, do not have improved insulation measures that became prevalent after the oil crisis in the early 1970s. After 1991, stricter regulations were imposed on building insulation. Additionally, computer-aided design methods improved the design of heating systems. Consequently, heating systems in the period after 1991 are often smaller compared to the previous periods (i.e., before 1974, and 1974–1991).

A sample of 220 buildings, covering different typologies and construction periods, is selected based on national statistics [17]. In this study, buildings are only considered if they are heated by gas heaters. Buildings with other heat sources are excluded from the sample. Feenstra staff made a selection from their gas boiler monitoring database, based on the above-mentioned criteria, and visited these clients to screen the suitability of the dwelling to participate in the experiment. Buildings were excluded from the sample if they had hydraulically unbalanced floor heating or lacked a plug connection near the gas boiler.

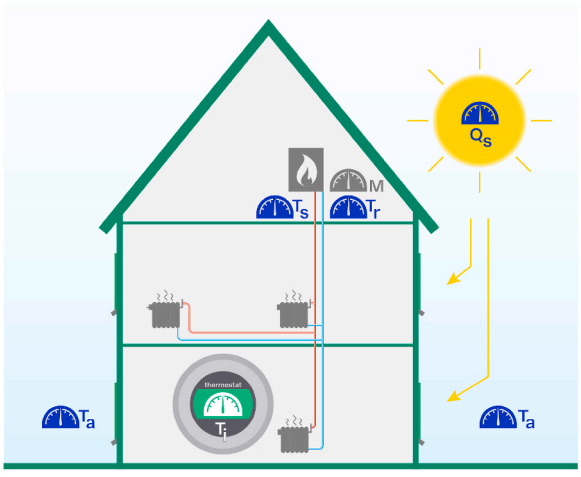

Fig. 1. Schematic of the experimental set-up for the dynamic integrated co-heating test of individual buildings. The gas heater is equipped with temperature sensors (T_s, T_r) and a flow meter (m). The indoor temperature (T_i) is monitored with the central thermostat. Ambient temperature (T_a) and solar influx (Q_s) are obtained from nearby weather station.

Table 1
Percentages of Dutch building stock per type and construction period (Top: CBS data 2016; Bottom: Sample).

Category	Detached	Corner	Terraced	Appartement	Total	
Before 1974	7.3	10.9	12.6	24.1	**54.9**	National reference
1974–1991	2.5	5.9	9.5	6.3	**24.2**	
After 1991	3.6	4.7	7.1	5.5	**20.9**	
Total target	**13.4**	**21.5**	**29.2**	**35.9**	**100**	
Before 1974	8.6 (+1.3)	12.7 (+1.8)	14.5 (+1.9)	14.5% (-9.6)	**50.4 (-4.5)**	Sample
1974–1991	2.7 (+0.2)	9.1 (+3.2)	11.4 (+1.9)	6.4% (+0.1)	**29.5(+5.3)**	
After 1991	3.2 (-0.4)	5.0 (+0.3)	7.7 (+0.6)	4.1% (-1.4)	**20.0 (-0.9)**	
Total realised	**14.5 (+1.1)**	**26.8 (+5.3)**	**33.6 (+4.4)**	**25.0 (-10.9)**	**100**	

The plug connection was required for the installation of the monitoring equipment. Furthermore, information on the type and size of all heating elements was collected during these screening visits.

Table 1 shows the target distribution in the Netherlands and the distribution of the sample set. The sample distribution deviates from the target distribution because of the exclusion criteria mentioned above. Old apartments (before 1974) are underrepresented and terraced and corners dwellings from the construction period 1974–1991 are overrepresented.

2.2. Measurement set-up

Fig. 1 shows the experimental set-up, that is based on the integrated co-heating test (i.e., energy meter method) [18,19]. The integrated co-heating test evaluates the thermal performance of a building and the heat emitted by the heating system. In this study, a dynamic integrated co-heating test has been used. Building properties, such as the heat loss coefficient of the building, the thermal inertia of the building envelope, and the lumped internal thermal inertia of a building (i.e., the thermal storage inside the building envelope), can be determined with the dynamic test. The dynamic integrated co-heating test requires data, such as the outdoor temperature, the indoor temperature, and the heat emitted by the heating system.

A data acquisition system (Leiderdorp Instruments, ElliTrack-N) is installed near the gas heater of each building in the sample. Data is transferred daily via a GSM-connection from the acquisition system to the database. The data is acquired at a 1-min interval but resampled to a 10-min interval. The heat flow to the heating system is accurately measured with two clamp-on temperature sensors (i.e., NTC thermistors) and a pulse flow meter (Honeywell, S110 PICOFLUX).

The clamp-on temperature sensors are installed near the gas heater on the supply and return pipe of the heating system. The NTC-sensors have an accuracy of $\pm 0.2\,^{\circ}C$. The pulse flow meter is installed near the gas heater on the supply pipe of the heating system. The pulse flow meter measures discharge up to a maximum flowrate of 3.0 m^3/h with an accuracy of 5% and a starting flow of 8×10^{-3} m^3/h.

The data acquisition system of the gas heaters (managed by Feenstra) measures the indoor temperature, and the temperature setpoint of the gas heater. The indoor temperature is measured with the central thermostat of the building. Data from the gas heater is stored in a database at irregular intervals. Consequently, the gas heater data is resampled to a 10-min interval by interpolation or averaging.

The natural-gas consumption is derived from data acquired by the acquisition system of the gas heaters. The (rotation) frequency of the ventilator is used to estimate the natural-gas consumption. The estimate of the natural-gas consumption is less accurate when there are many start-up and shutdown cycles. It is noted that the estimate of the natural-gas consumption is only used to determine the annual and specific annual gas demand for space heating.

The outside temperature and solar influx are, for each building, obtained from data collected at a nearby weather station. The weather station "Deelen" of the Royal Dutch Meteorological institute (KNMI) is geographically closest to most of the buildings in the sample. The data from the weather station is imported at an hourly interval. Thereafter, the data is resampled to a 10-min interval.

2.3. Modelling approach

Grey box models combine an incomplete theoretical model with measurement data. For buildings, a theoretical model with a combination of lumped resistances (R) and capacitors (C) is often combined with measurements of the indoor temperature. These $n_R Rn_C C$-models increase in complexity with more resistances (i.e., n_R) and capacitors (i.e., n_C).

For example, the parameter estimation of a third order model with three state variables (i.e., indoor temperature (T_i), wall temperature (T_e) and radiator temperature (T_h)) may result in unrealistic resistance and capacitance values. The larger number of state variables with a single observed variable result in identifiability problems, see for example [20], and increased model parameter uncertainty [21]. The parameter uncertainty can be reduced by supplementing the model with observed solar irradiation data [21]. In this study, a second order building model (2R2C) is used with one observed variable (i.e., indoor temperature).

Fig. 2 shows a schematic of the second order building model. The model solves a system of two ordinary differential equations (ODE) over time. Equation (1) models the temporal variation of the indoor temperature (T_i) and is given by:

$$\frac{dT_i}{dt} = \frac{1}{R_{ie}C_i}(T_e - T_i) + \frac{Q_h}{C_i} + \frac{A_w Q_s}{C_i} \tag{1}$$

with the thermal resistance between the interior and the building envelope (R_{ie}), the internal capacitance (C_i), the building envelope temperature (T_e), the heat supplied by the heating system (Q_h), the effective surface area for solar irradiation (A_w), and the heat supplied by solar irradiation (Q_s). Equation (2) models the temporal variation of the building envelope temperature and is given by:

$$\frac{dT_e}{dt} = \frac{1}{R_{ie}C_e}(T_i - T_e) + \frac{1}{R_{ea}C_e}(T_a - T_e) \tag{2}$$

with the external capacitance (C_e), the thermal resistance between the building envelope and the external surrounding of the building (R_{ea}), and the ambient temperature (T_a).

An open-source tool for nonlinear programming, CasADI [22] with the Ipopt solver [23], is used to calibrate the second order building model. The building model is calibrated by minimizing the

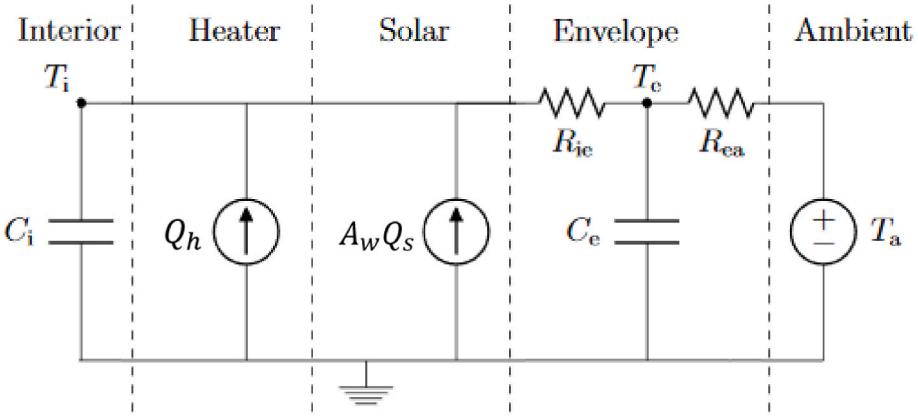

Fig. 2. Electric analogy of the 2R2C building model (source [20]):

root-mean-square error (RMSE) of the indoor temperature. For each building in the sample, three 10-day periods are selected from the data for which the average ambient temperature is the lowest. An extra condition is imposed on the data, that all data should be available for each 10-day period. The model is trained on two of the three 10-day periods. The remaining period is used to validate the model and to prevent overfitting.

The grey-box model is a simplified model to estimate the day-night behavior of a complete building. The least squares method will minimize the residual error of the indoor temperature. The minimization will compensate for model and measurement uncertainties, which may result in over- and/or underestimation of the building parameters. There are several uncertainties that should be addressed, namely: the uncertainty of the input data and the uncertainty of the model assumptions.

The uncertainty of the input data can, amongst others, be attributed to measurement errors and the weather data. The measurement data could be biased by local processes. For example, the building thermostat can measure higher temperature when there is direct solar irradiation on the sensor. Additionally, the measurement data is sampled at a higher frequency and down sampled to the model frequency. The down sampled measurement data has a lower error for processes with a lower frequency than the model frequency. However, hourly processes (i.e., short-term, and high frequency) are not well represented by the model.

The weather data is collected at the nearest weather station, which could be quite far from the actual location of the building. There is no correction in the model for local weather conditions, such as cooling by wind. Consequently, the temperature in the model was not corrected for wind due to lack of (more) local weather data.

2.4. Design heat output

The minimum design supply temperature of the heating system ($T_{s,d}$) in each dwelling in our sample is based on the design heat output $Q_{h,d}$ and corresponding measured supply (T_s), return (T_r), and indoor (T_i) temperature. This method consists of two steps. First, the design heat output is derived from the calibrated resistance values in the grey box model. Secondly, the minimum required supply temperature is derived from the available monitoring data.

In the Netherlands, the design condition is defined at a daily-average ambient temperature of $T_a = -10\,^{\circ}C$ without solar irradiation ($Q_s = 0$) and an indoor temperature of $T_i = 20\,^{\circ}C$. The calibrated grey-box model (Eq. (1) and (2)) defines the steady heat output at this condition (Eq. (3)).

$$Q_h = \frac{(T_i - T_a)}{R_{ie} + R_{ea}} \tag{3}$$

If we would adopt this steady heat supply as the design heat supply, then the heating system would be in operation full time (24 h) at design load during a day with design weather conditions. In that case, there would be no safety margin or time to prepare hot tap water from the same heat source. Therefore, we make an important assumption that the design heat output $Q_{h,d}$ is supplied in 18 h, which corresponds with a 33% safety margin on the steady heat output. This assumption aligns with a future-proof design of low-temperature heating systems, while accounting for modelling uncertainties and time to fill a buffer for domestic hot water.

2.5. Minimum supply temperature at design condition

The heat output to the radiator system is, for quasi-steady conditions, given by:

$$Q_h = h(T_s)A\Delta T_{LMTD} = \dot{m}c_p\Delta T_{sys} \tag{4}$$

with the temperature dependent heat transfer coefficient of the radiators $h(T_s)$, the surface area of the radiators A, the log-mean temperature difference ΔT_{LMTD}, the mass flow rate to the radiators $\dot{m}$, the specific heat capacity of the fluid in the radiator system c_p, and the temperature difference over the radiator system ΔT_{sys}. The temperature difference over the radiator system is defined as $\Delta T_{sys} = T_s - T_r$ with T_s as supply and T_r as return temperature. The log-mean temperature difference is defined by equation (5).

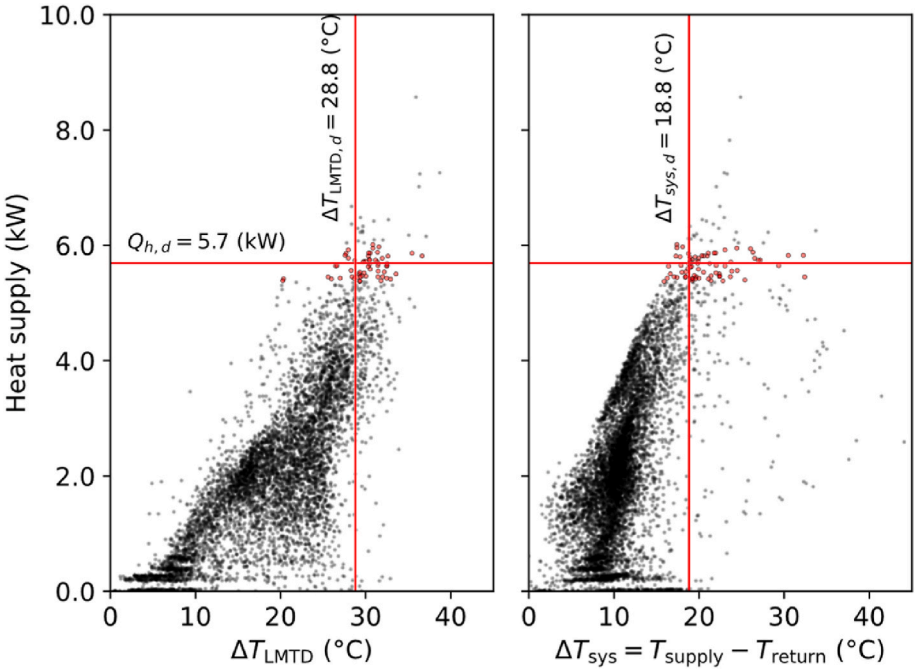

Fig. 3. Hourly-averaged and flow weighted data: (a) the measured log-mean temperature difference (ΔT_{LMTD}) versus the heat supply to the system (Q_h); (b) the measured temperature difference over the radiator system (ΔT_{sys}) versus the heat supply to the system (Q_h). The horizontal line depicts the design heat output ($Q_{h,d}$) at design conditions from the grey-box model. 1% of the data-points closest to the design heat output are shown as red dots. The vertical lines depict the design log-mean temperature difference ($\Delta T_{LMTD,d}$) and the design temperature difference over the radiator system ($\Delta T_{sys,d}$).

$$\Delta T_{LMTD} = \frac{\Delta T_s - \Delta T_r}{ln\left(\frac{T_s - T_i}{T_r - T_i}\right)} = \frac{T_s - T_i - (T_r - T_i)}{ln\left(\frac{T_s - T_i}{T_r - T_i}\right)} = \frac{T_s - T_r}{ln\left(\frac{T_s - T_i}{T_r - T_i}\right)} = \frac{\Delta T_{sys}}{ln\left(\frac{T_s - T_i}{T_r - T_i}\right)} \quad (5)$$

The log-mean temperature difference and the temperature difference over the radiator system are directly computed from the measured supply, return, and indoor temperature.

The data-driven method to determine the design supply temperature is illustrated in Fig. 3 for one dwelling, which shows the hourly-averaged and flow-weighted data of the log-mean temperature difference (ΔT_{LMTD}) and the temperature difference over the radiator system (ΔT_{sys}) versus the heat supplied (Q_h) by the radiator system. The data is hourly-averaged to remove the effect of short-term dynamics (i.e., heating of the radiator). These short-term dynamics are not representative for the heat transfer to the building interior. The temperature data is flow-weighted, which automatically excludes data during no flow conditions. The horizontal line shows the design heat output of this dwelling. The design heat output is frequently exceeded in the morning due to the night setback operation, which was applied in almost all dwellings. A data slice is selected that includes 1% of the data that is closest to the design heat output ($Q_{h,d}$).

Each heat output is delivered at range of temperature differences (i.e. ΔT_{LMTD} and ΔT_{sys} in Fig. 3) due to part-time operation and variable mass flow rates. We are looking for the smallest hourly-averaged temperature differences that deliver the design heat output. Therefore, the log-mean temperature difference and temperature difference over the radiator system at design conditions (i.e., $\Delta T_{LMTD,d}$ and $\Delta T_{sys,d}$) are defined by the 25% percentile values of the monitoring data at the design heat output. These 25% percentile values of log-mean and system temperature difference are indicated with the vertical lines in Fig. 3. The 25%-percentile value in Fig. 3a) represents a data point with the highest feasible heat transfer coefficient, while delivering the design heat output. It is noted that the power-law-relation of the radiator coefficient is poorly visible in the experimental data of all dwellings. Data points at higher percentile values of the log-mean temperature difference and the same heat output correspond with smaller heat transfer coefficients and probably smaller mass flow rates. The 25%-percentile value in Fig. 3b) represents a data point close to the largest feasible mass flow rate. Data points at higher percentile values of the system temperature difference ΔT_{sys} must correspond with smaller hourly-averaged mass flow rates according to equation (4). These 25% percentile values are considered the minimum feasible temperature differences to deliver the design heat output.

These two temperature differences, $\Delta T_{LMTD,d}$ and $\Delta T_{sys,d}$, are combined to obtain the minimum supply temperature of the heating system at design conditions ($T_{s,d}$) following some algebraic manipulation of Eq. (5), resulting in Eq. (6). The return temperature of the radiator system at design conditions follows immediately from $T_{r,d} = T_{s,d} - \Delta T_{sys,d}$. For the example data in Fig. 3, the log-mean temperature difference at design conditions is $\Delta T_{LMTD,d} = 28.8\,^{\circ}C$, whereas the temperature difference at design conditions is $\Delta T_{sys,d} = 18.8\,^{\circ}C$. Consequently, the minimum supply temperature at design conditions (Eq. (6)) is $\Delta T_{s,d} = 59.2\,^{\circ}C$ for the building with anonymized identifier number 20051101.

$$T_{s,d} = T_i + \frac{\Delta T_{sys,d}}{1 - e^{-\left(\frac{\Delta T_{sys,d}}{\Delta T_{LMTD,d}}\right)}} \quad (6)$$

The method to determine the minimum supply temperature at design conditions contains several implicit sources of uncertainty. First, the heat output at the design condition is derived from a calibrated grey-box model. We account for some uncertainty in both the model data as well as the measurement data by considering 1% of the data closest to the design heat output ($Q_{h,d}$). Second, the flow-weighted hourly average of the temperatures is used to determine the design temperature at the design condition. Short-term dynamics are therefore not affecting the estimated minimum supply temperature at design conditions.

2.6. Oversizing factor

The oversizing factor describes the ratio of the installed heat output ($Q_{h,a}$) over the design heat output ($Q_{h,d}$) [13]. In this study, the inverse of the oversizing factor is defined as the dimensionless design heat output (Eq. (7)). The dimensionless design heat output might indicate the potential for lower-supply temperatures of a heating system in individual buildings.

$$\eta = \frac{Q_{h,d}}{Q_{h,a}} \quad (7)$$

An estimate of the installed heat output ($Q_{h,a}$) is derived by summing design heat outputs of individual radiators, derived from generic, simplified correlations, based on the available data acquired during the screening visits: type of heating element and relevant dimensions. The radiators in our sample are divided into three categories, namely panel, column, and design radiators. The heat output of each radiator is derived from a correlation that is type dependent. The reference temperatures for supply, return and indoor temperature to determine the design heat output are 75/65/20 °C.

The heat output of a panel radiator is estimated for several sub-types (i.e., 10, 11, etc.). The heat output is defined by equation (8) with the length (L) and height (H) of the panel combined with two constants (i.e., A and B) that depend on the sub-type (see Table 2). The heat output of design radiators is also defined by equation (8) with conservative parameter values (see Table 2).

$$Q_a = (A + BH)L \quad (8)$$

The heat output of column radiators is derived from the surface area of the columns in the radiator (A_c) multiplied with a conservative constant 0.65 kW/m^2. The surface area of the columns is defined by the number of columns (N_{col}) with their respective column height (H) and width (W) (Eq. (9)).

$$A_c = N_{col}HW \quad (9)$$

For the buildings in our sample, the radiator type and dimensions were recorded during site visits. The radiator types in our sample are divided in approximately 87.4% panel, 3.5% column and 7.8% design radiators. The heat output from convector radiators was neglected, due to their limited presence in the sample (i.e., 1.3% of installed radiators). The buildings in our sample have on average 8.5 radiators.

3. Results

3.1. Annual and specific heat demand of sample

The specific head demand and gas consumption of our sample are compared with available data from the province of North Holland (Servicepunt Duurzame Energie) combined with data from the Dutch national statistics agency (CBS). The specific heat demand (kWh/(m^2 yr)) defines the heat loss from a building during a year over the total (livable) surface area of that building. The available data is divided into single- and multi-family homes. The detached, corner, and terraced

Table 2
The constants (i.e., A and B) of equation (7) are presented for different sub-types of the panel radiator. The values of the design radiator are also tabulated.

Panel type	Parameter A [kW/m]	Parameter B [kW/m^2]
10	0.08	0.88
11	0.10	1.43
20	0.15	1.45
21	0.20	1.81
22	0.30	2.16
33	0.45	3.07
Design	0.06	0.51

Table 3
Average specific heat demand for space heating (SH) in Dutch residential buildings. Data from Ref. [24] and national statistics (CBS). Data is aggregated to the construction periods of the current study.

Homes	Construction period	Average floor area [m^2]	Average gas consumption for SH [m^3]	Average specific heat demand SH [kWh/(m^2yr)]
Single family homes	before 1974	166	1729	97
	1974–1991	130	1390	75
	after 1991	149	1108	54
Multi-family	before 1974	79	1164	92
	1974–1991	70	840	70
	after 1991	90	726	45

dwellings are therefore aggregated to the category single-family homes.

Table 3 shows the average specific heat demands of dwellings in the Netherlands. Table 4 shows the average specific heat demands of the dwellings in this study. For each building in the sample, the specific heat demand is derived from gas consumption data combined with the surface area. The specific heat demand of our sample is on average larger than that of the Netherlands. There are several reasons for this deviation.

First, the age distribution in the most recent construction period of the sample (i.e., after 1991) is skewed towards older houses. The buildings in this period are on average constructed in the year 2000 for single-family and 1998 for multi-family homes. The newest buildings in the sample are for both single- and multi-family homes constructed in 2009. The skewed age distribution of our dwellings causes much larger specific heat demands in our sample; 59% larger for single family dwellings and 96% larger for multi-family buildings.

Second, the specific heat demand in the sample is based on gas consumption data from 2021. In the Netherlands, the year 2021 was on average cold compared to the last 3 decades. Consequently, there were approximately 140 additional heating degree days (HDD) compared to the average of the last 3 decades (2800 °Cday), which would explain 5% difference. The average specific heat demand of all dwellings in our sample, constructed before 1992, is 12% tot 28% larger than the specific heat demand in available statistics.

The sample does not account for individual behavior such as night setbacks, the amount of ventilation, and the number of heated rooms in a building. Furthermore, people spent more time at home during the Corona pandemic due to travel restrictions and lockdowns. Consequently, there is some variation in the sample compared to the average of the Netherlands due to individual behavior that is not accounted for in the current sample.

3.2. Model calibration results

The grey-box model is successfully calibrated for 187 of the 220 buildings in the sample. There were three reasons for an unsuccessful calibration. First, the model could not be calibrated and validated when the required 10-day periods were incomplete. Second, the data acquisition system was no longer available during the required period. In some cases, the inhabitants of the building disconnected the data acquisition system. Finally, two buildings were excluded after model fitting, because the extreme design heat output values of 29 W and 41 kW were considered outliers.

Table 4
Average specific heat demand for space heating (SH) in the sample. The last column includes in brackets the percentual difference with the values in Table 3.

Homes	Construction period	Average floor area [m^2]	Average gas consumption SH 2021 [m^3]	Average specific heat demand SH 2021 [kWh/(m^2yr)]
Single family	before 1974	135	1596	110 (+12%)
	1974–1991	142	1332	87 (+28%)
	after 1991	129	1222	88 (+59%)
Multi-family	before 1974	83	974	109 (+19%)
	1974–1991	73	756	96 (+25%)
	after 1991	93	856	86 (+96%)

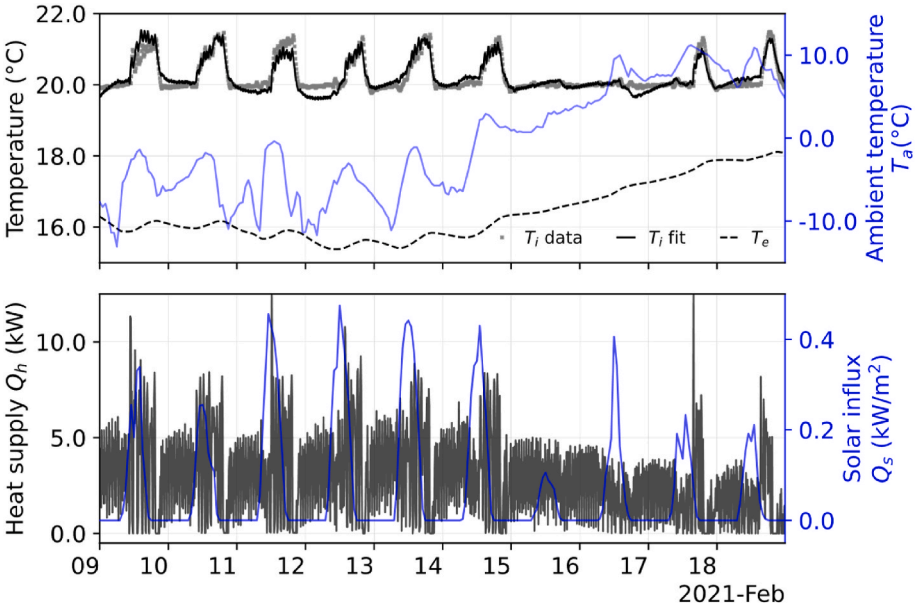

Fig. 4. Combined plot of the validation data and model fit of the indoor (T_i) and envelope (T_e) temperature for the coldest 10-day period in 2021. The results of the fitted 2R2C model of anonymized building 20,051,101 are shown. Note that the ambient temperature (T_a) is plotted in blue on the right vertical axis.

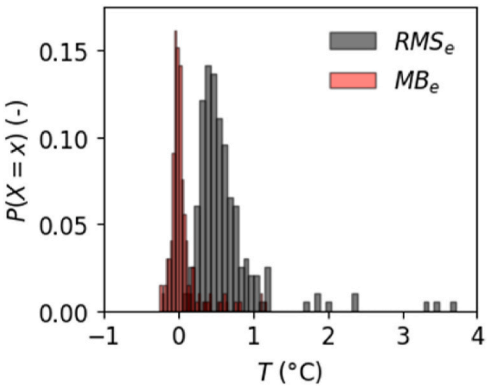

Fig. 5. Error histograms for the validation period. Mean bias is shown in pink, RMSE is shown in grey.

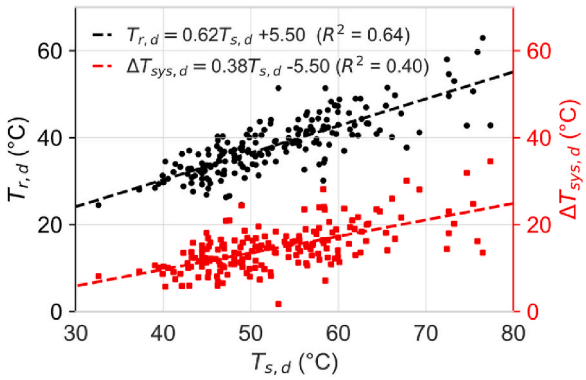

Fig. 6. Relation between design supply temperature ($T_{s,d}$) and both the design return temperature ($T_{r,d}$) and temperature difference of the radiator system ($\Delta T_{sys,d}$) for all buildings of the sample. The shown data is derived from the calibrated grey-box models of each individual building.

Fig. 4 shows an illustrative 10-day training period for a building with anonymized identifier number 20051101. The indoor temperature is accurately predicted with an RMSE of 0.15 °C over the 10-day validation period. The model shows a reasonable agreement between the measurement data (i.e., grey dots) and the model prediction (i.e., black line) of the indoor temperature (T_i).

The trained model has an average RMSE of the indoor temperature (T_i) of 0.44 °C for the training data and 0.54 °C for the validation data (Fig. 5). The average error or bias between modelled and measured indoor temperature in the training period is as low as −0.0025 °C with a standard deviation of 0.005 °C. The bias in the validation period is 0.04 °C with a standard deviation of 0.2 °C (Fig. 5). This indicates that the resistance values are accurately calibrated because the thermal resistance values determine the bias in the indoor temperature. It is emphasized that these calibrated resistance values of the grey-box model are used to determine the design heat output as detailed in section 2.4.

3.3. How low can we go?

The reduced supply and return temperatures have been determined for 178 dwellings. The reduced supply and return temperature could not be determined when all hourly-averaged heat output data points were well below the design heat output. These inhabitants applied a constant indoor temperature setpoint without night-setback.

Table 5 shows the average design properties of the 178 dwelling that were successfully calibrated. The design supply temperature ($T_{s,d}$) is on average 53.1 °C with a standard deviation of 8.7 °C. The design supply temperature can be lower than 49.6 °C for 40% of the buildings in the sample. Moreover, a design supply temperature of 55.3 °C could be sufficient for 60% of the buildings in the sample. Following Dutch definitions of low-temperature heating (Ts < 55 °C), these results suggest that 60% of the existing residential homes in the Netherlands is LT-ready.

A medium-temperature (MT) heating system operates at a supply temperature lower than 70 °C. In the current sample, the design supply temperature could be lower than 70 °C for 95% of the buildings. The percentage of buildings in the Netherlands that is MT-ready might even be higher than 95%, if buildings with other heat sources and floor heating would be included in the sample.

The design return temperature ($T_{r,d}$) and design temperature difference over the radiator system ($\Delta T_{sys,d}$) are important control parameters for gas heaters and district heating systems. Fig. 6 shows the design return temperature and design temperature difference over the radiator system as a function of the design supply temperature. The results show that the design return temperature is linearly related to the design supply temperature with $R^2 = 0.62$ (Fig. 6). The design temperature difference over the radiator system shows a weaker linear relationship with the design supply temperature ($R^2 = 0.4$).

In this study, the average design temperature difference is 15 °C (at $T_{s,d}/T_{r,d} = 53/38$) with only 20% of the dwellings exceeding a temperature difference of 18 °C (60/42). Hence it seems difficult to achieve system temperature differences of 20 °C (50/30) or 30 °C (55/25) as recommended for LT district heating [25].

Table 5
Statistics of the supply temperature, return temperature and temperature differences during design conditions of the 178 buildings in the sample.

Design properties	Mean value (°C)	Standard deviation (°C)	Percentiles				
			20th	40th	60th	80th	95th
supply temperature ($T_{s,d}$)	53.1	8.7	45.3	49.6	55.3	59.5	69.7
return temperature ($T_{r,d}$)	38.5	6.8	32.6	36.5	40.2	43.3	50.4
System temperature difference ($\Delta T_{sys,d}$)	14.6	5.1	10.5	12.9	15.2	18.1	23.9
Log-mean temperature difference ($\Delta T_{LMTD,d}$)	25.0	7.4	18.3	22.5	26.5	30.8	37.5

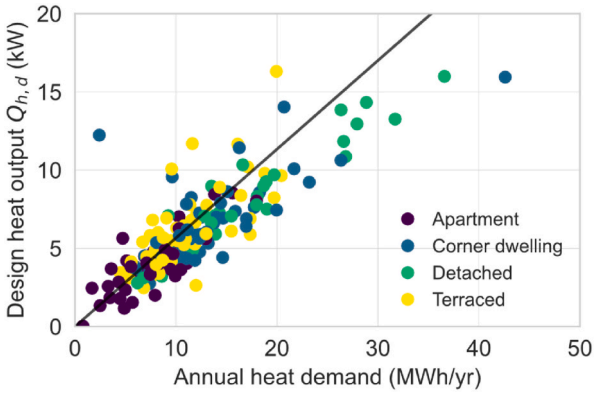

Fig. 7. Annual heat demand (E_s) versus the design heat output ($Q_{h,d}$). The continuous line shows equation (9) as $Q_{h,d} \approx 0.57\, E_s$ with the annual heat demand as E_s [MWh/yr].

3.4. Exploratory analysis LT-ready metric

Based on the result of this study that 60% of the Dutch residential building stock is LT-ready, it would be beneficial to home owners, housing corporations, installation companies and district heating companies to develop a metric for LT-readiness. The results are analyzed in more detail to identify which parameters could predict the minimum supply temperature. A metric to determine whether a building is LT-ready, is preferably based on easily available parameters, such as the construction period, building typology or annual heat demand.

Fig. 7 shows the design heat output versus the annual heat demand (E_s) for space heating per building category. The design heat output versus the annual heat demand shows a linear tendency, which is expected according to engineering design rules. Equation (9) shows a design rule based on the number of heating degree days at the design condition HDD_d , the total number of heating degree days (HDD), and the number of full load hours ($t_{Q,d}$) during the design day. This design rule is a more specific version of the HDD-scaling as proposed by Ref. [11]. For example, a specific annual heat demand of 20 MWh/yr, at the design conditions in the Netherlands (i.e. $HDD_d = +\ 20 - (-10) = 30\ ^\circ Cday$), $HDD = 2940^\circ Cday$, and $t_{Q,d} = 18$ h, requires a design heat output of $Q_{h,d} = 11.3$ kW (see Fig. 7).

$$Q_{h,d} = \frac{HDD_d}{HDD}\frac{1}{t_{Q,d}} E_s \tag{10}$$

It is emphasized that the datapoints in Fig. 7 stem from different sources. The data on the design heat output is derived from the calibrated grey-box models of each individual building. On the other hand, the data from the annual heat demand is derived from the indirect measurement of gas consumption. Consequently, the correlation in Fig. 7 is not an artefact of the analysis.

Another potential parameter to predict the minimum supply temperature is the specific heat demand. Fig. 8 shows the design supply temperature versus the specific heat demand for both the building type and construction period. There is no obvious linear trend between the design supply temperature and the specific heat demand. Furthermore, Fig. 8 does not directly indicate a relation between supply temperature and building type or construction period. Nonetheless, it is interesting to note that appartements in this sample do not necessarily have a smaller specific heat demand than the other building types. The lower gas consumption of appartements compared to other buildings can be mainly attributed to the variation in average floor area, as shown in Table 4.

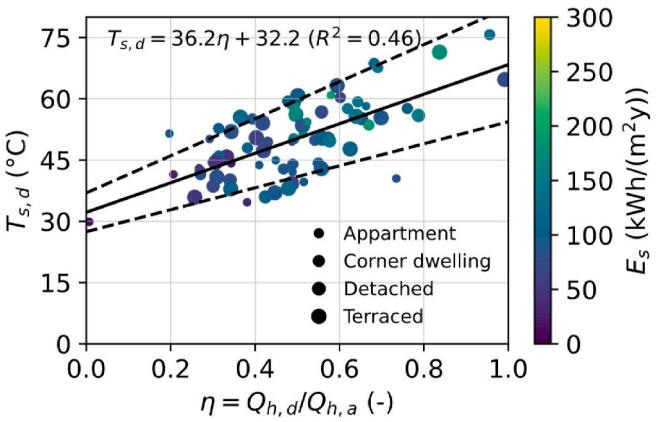

Fig. 9. Dimensionless design heat output (η) versus the design supply temperature ($T_{s,d}$), which indicates a linear trend of $T_{s,d} = 36.2\eta + 32.2$ for the aggregated data. The marker color shows the specific annual heat demand, whereas the marker size shows the building type. The shown data is derived from the calibrated grey-box models of each individual building.

The data indicates substantial variation for all building types and construction periods (see Fig. 8). There are several buildings in the construction period before 1974 with a design supply temperature lower than 50 °C. In addition, the specific heat demand of the buildings in this period varies between $50 \leq E_s \leq 250$ kWh/(m^{2}yr). The variation in specific heat demand and supply temperature is similar for all construction periods. The variation could be attributed to occupant behavior and improvements of the building envelope over time (i.e., cavity wall insulation, double-glazed windows, etc.).

The correlation between design supply temperature and the dimensionless design heat output (η), defined in Eq. (7), is shown in Fig. 9. A linear relation ($R^2 = 0.46$) can be identified between the supply temperature and the dimensionless design heat output. Accordingly, the dimensionless design heat output could indicate the LT-readiness of a building. For example, a design supply temperature of $T_{s,d} \leq 55\ ^\circ C$ could already be obtained with a dimensionless design heat output of $\eta \leq 0.63$. Occupant behavior, like ventilation habits and the number of rooms with closed radiators, may contribute to the variation in the reduced design supply temperature.

This exploratory analysis suggests that the dimensionless design heat output is a promising parameter to predict the minimum design supply

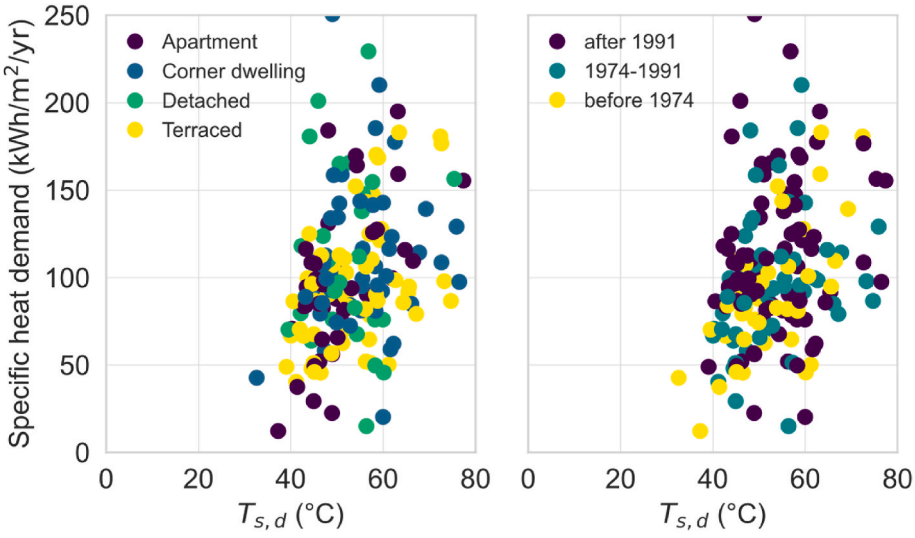

Fig. 8. The design supply temperature versus the specific heat demand for the building in the sample. (a) Colors indicate building type. (b) Colors indicate construction period.

temperature of a dwelling and confirms the relevance of the radiator oversizing for LT-readiness [4,9,12]. The dimensionless design heat output requires information on the design heat output and the installed heat output of all heating elements in the dwelling following Eq. (7). The design heat output can be based on the annual heat demand, using Eq. (10), and the installed heat output can be easily determined for an individual dwelling, based on specifications of the heating elements or Table 2. Unfortunately, the installed heat output is not readily available in national databases. Finally, the exploratory analysis shows that the widely available parameters (building type, construction period and specific heat demand) are poorly correlated with the minimum design supply temperature.

4. Discussion

The current method to determine the coefficients of the grey-box model has several shortcomings. First, the model coefficients are determined without altering the behavior of the building inhabitants. Consequently, the accuracy of the predicted thermal inertia is limited in dwellings with limited indoor temperature variation during calibration periods. The results could be improved by advising a night setback during calibration periods. Second, the current model structure uses two thermal resistance values, to model conduction through the building envelope. The grey-box model structure could be refined with wind-driven infiltration losses, although the risk of identifiability problems may increase. Finally, the model is calibrated with measurement data from gas-fired heating systems in existing buildings. These gas heaters are not designed to modulate to small, future-proof, heat outputs, while the model is used to determine future-proof design conditions that require more full-load hours at moderate heat outputs.

The coefficients of the grey-box model could be determined with another method to improve the accuracy of the building model. A two-step approach is proposed to improve the estimate of the model coefficients by accounting for the difference in timescale of the thermal inertia versus thermal resistance. In the first step, the daily average of the measurement data could be used to derive the thermal resistance of the model. Thereafter, the high-frequency measurement data combined with the initial estimate of the thermal resistance should be used to determine the thermal inertia. The two-step calibration approach could improve the accuracy of a model with different timescales.

A detailed study of the building model parameters was not performed. Nonetheless, the thermal inertia derived from the building could be used to develop future-proof demand response strategies. These demand response strategies are required for affordable smart energy systems. The future-proof demand response strategies allow for matching of heat production from renewable sources with heat demand.

The results on the design temperature difference for space heating require some reflection. Avervalk et al. [25] propose temperature differences of 20 °C (50/30) or 30 °C (55/25) for low-temperature district heating, while our results suggest a design temperature difference of 15 °C (55/40) to 24 °C (70/50) with hydraulically balanced heating systems. A larger system temperature difference can be theoretically obtained by increasing the supply and lowering the return temperature to maintain the same log-mean temperature difference. The system temperature also increases by accounting for the domestic hot water consumption, which has not been addressed in this study. Therefore, temperature differences of 20 °C–30 °C seem feasible in the Netherlands. This statement is supported by practical experiences. Dutch district heating company HVC performed measurements with reduced supply temperatures in a neighborhood with 500 dwellings, constructed in the 1980s. The field measurements were performed during a cold spell in February 2021, for which a 10-day period is also shown in Fig. 4. The average measured supply and return temperature were 67 $^{\circ}C$ and 42 $^{\circ}C$ in the buildings connected to the district heating network. This confirms that 25 $^{\circ}C$ temperature difference is feasible in district heating grids with supply temperatures just below 70 °C.

The sample in this study is representative for the dwellings in the Netherlands based on the building construction period and the building type. The average specific heat demand in our sample is larger than the national average specific heat demand per class of building type and construction period. This suggests that the percentage of dwellings that is LT-ready might even be larger than 60%. However, the representativeness of the occupants in the sample was not considered. Individual occupant behavior could influence the measurements and thereby the reduced design supply temperature. A larger sample of participants that are representative for the dwellings in the Netherlands could be considered to generalize the conclusions of this study.

This study has shown that a significant fraction of the Dutch building stock is LT-ready if the proposed assumption on future-proof design of LT heating systems is adopted. This conclusion may have a significant impact on the required investments to decarbonize the heat supply to residential areas. Individual buildings and district heating grids may transform more cost-effectively from HT to LT-operation. It seems unnecessary to invest in underfloor heating or LT-radiators to adopt LT-heating, especially in combination with additional insulation measures to reduce the heat demand for space heating.

The dimensionless design heat output (η) could be used to determine the LT-readiness of a dwelling. Caution must be exercised when using the minimum supply temperature derived from the dimensionless design heat output. In this study, the heating system of each dwelling was hydraulically balanced before installing the monitoring equipment. Furthermore, the supply temperature of the heating system was lowered to the recommended value by a service technician. Afterwards, the behavior of the gas heater and the perceived thermal comfort were monitored. Consequently, the supply temperature of a gas heater should not be lowered without consulting a service technician.

5. Conclusions

A representative sample of 220 dwellings in the Netherlands of different building types and construction periods, is selected based on national statistics. All dwellings in the sample are heated with gas heaters.

All buildings in the sample are equipped with a novel monitoring system that acquires the indoor temperature, supply and return temperature of the gas heater, and the flow rate to the heating system. The measurement data is supplemented with weather data from a nearby weather station and (historical) gas consumption data from the gas heater.

A novel fully data-driven approach to determine the minimum required supply temperature during design conditions has been developed, including a grey-box 2R2C building model and the assumption that 18 full-load hours are required on the design day. The indoor temperature (T_i) is accurately predicted by the model with an average bias of 0.04 °C and RMSE equal to 0.54 °C for the validation period.

The data-driven method indicates that nearly all buildings in the sample (i.e., 95%) can be heated with supply temperatures lower than 70 $^{\circ}C$. Moreover, the design supply temperature can be reduced to 55 $^{\circ}C$ or lower in 60% of the dwellings. The data shows a linear relation between the design heat output and the annual heat demand for space heating. There is no clear relation between the building type, construction period or specific annual heat demand and the design supply temperature. The exploratory analysis suggests that the ratio between the required and installed heat output of the radiators is a promising LT-readiness metric to predict the minimum design supply temperature of an individual dwelling. The required heat output in this LT-readiness metric can be estimated from the annual heat demand as proposed by Eq. (10).

CRediT authorship contribution statement

D. Vreeken: Development of grey-box model, Analysis,

M. van Meerkerk: Analysis, Writing – review & editing.

I. Pothof: Conceptualization of the study, Methodology, Analysis, Writing – original draft, revision.

Declaration of competing interest

The authors declare that they have no known competing financial interests or personal relationships that could have appeared to influence the work reported in this paper.

Data availability

Data will be made available on request.

Acknowledgements

This research has been carried out as part of the WarmingUP programme, co-funded by the Dutch Ministry of Economic Affairs and Climate Policy (grant nr. TEUE819001). We kindly acknowledge the support by Andrea Forzoni for the organizational support, Martijn Smeulers for setting up the data-acquisition and MSc student Max Coenen for co-developing the experimental set-up. We also thank Ronald Pilot and Ton van den Berg from the installation company Feenstra BV for helping us get a representative sample of existing buildings in the Netherlands. Their work was complicated by the COVID-19 pandemic that passed the Netherlands during the project. Finally, we thank the district heating companies for their constructive feedback on the analysis and preliminary results: Martijn Matijssen (Vattenfall), Arjen Baltus (HVC), Berry de Jong (SVP), Niels van Schie (Eneco) and Richard van Ballegooijen (ENnatuurlijk).

References

[1] European Commission. Energy use in buildings. 2022. https://Ec.Europa.Eu/Energy/Eu-Buildings-Factsheets_en.

[2] European Council. 'Fit for 55': EU strengthens emission reduction targets for member states. 2022. https://Www.Consilium.Europa.Eu/En/Press/Press-Releases/2022/11/08/Fit-for-55-Eu-Strengthens-Emission-Reduction-Targets-for-Member-States/.

[3] Benakopoulos T, Vergo W, Tunzi M, Salenbien R, Kolarik J, Svendsen S. Energy and cost savings with continuous low temperature heating versus intermittent heating of an office building with district heating. Energy 2022;252. https://doi.org/10.1016/j.energy.2022.124071.

[4] Østergaard DS, Smith KM, Tunzi M, Svendsen S. Low-temperature operation of heating systems to enable 4th generation district heating: a review. Energy 2022;248. https://doi.org/10.1016/j.energy.2022.123529.

[5] Harrestrup M, Svendsen S. Changes in heat load profile of typical Danish multi-storey buildings when energy-renovated and supplied with low-temperature district heating. Int J Sustain Energy 2015;34(3–4):232–47. https://doi.org/10.1080/14786451.2013.848863.

[6] Rønneseth Ø, Holck Sandberg N, Sartori I. Is it possible to supply Norwegian apartment blocks with 4th generation district heating? Energies 2019;12(5):941. https://doi.org/10.3390/en12050941.

[7] Wang Q, Ploskić A, Holmberg S. Retrofitting with low-temperature heating to achieve energy-demand savings and thermal comfort. Energy Build 2015;109:217–29. https://doi.org/10.1016/j.enbuild.2015.09.047.

[8] Østergaard D, Svendsen S. Space heating with ultra-low-temperature district heating - a case study of four single-family houses from the 1980s. Energy Proc 2017;116:226–35. https://doi.org/10.1016/J.EGYPRO.2017.05.070.

[9] Jangsten M, Kensby J, Dalenbäck J-O, Trüschel A. Survey of radiator temperatures in buildings supplied by district heating. Energy 2017;137:292–301. https://doi.org/10.1016/j.energy.2017.07.017.

[10] Østergaard DS, Svendsen S. Experience from a practical test of low-temperature district heating for space heating in five Danish single-family houses from the 1930s. Energy 2018;159:569–78. https://doi.org/10.1016/j.energy.2018.06.142.

[11] Benakopoulos T, Tunzi M, Salenbien R, Hansen KK, Svendsen S. Implementation of a strategy for low-temperature operation of radiator systems using data from existing digital heat cost allocators. Energy 2022;251. https://doi.org/10.1016/j.energy.2022.123844.

[12] Østergaard DS, Svendsen S. Are typical radiators over-dimensioned? An analysis of radiator dimensions in 1645 Danish houses. Energy Build 2018;178:206–15. https://doi.org/10.1016/j.enbuild.2018.08.035.

[13] Reguis A, Vand B, Currie J. Challenges for the transition to low-temperature heat in the UK: a review. Energies 2021;14(21). https://doi.org/10.3390/en14217181.

[14] KNMI. KNMI Klimaatsignaal'21: hoe het klimaat in Nederland snel verandert. 2021.

[15] Nord N, Ingebretsen ME, Tryggestad IS. Possibilities for transition of existing residential buildings to low temperature district heating system in Norway. In: Proceedings of the 12th REHVAWorld congress; 2016.

[16] Netherlands Enterprise Agency (RVO). Voorbeeldwoningen 2011, bestaande bouw (in Dutch). 2011.

[17] Coenen MMG. Accelerating the Dutch energy transition: lowering operating temperatures of heat distribution systems in the built environment. Msc thesis. University of Groningen; 2019.

[18] Bauwens G, Roels S. Co-heating test: a state of- the-art. Energy Build 2014;82:163–72.

[19] Farmer D, Johnston D, Miles-Shenton D. Obtaining the heat loss coefficient of a dwelling using its heating system (integrated coheating). Energy Build 2016;117:1–10. https://doi.org/10.1016/j.enbuild.2016.02.013.

[20] Bacher P, Madsen H. Identifying suitable models for the heat dynamics of buildings. Energy Build 2011;43(7):1511–22. https://doi.org/10.1016/j.enbuild.2011.02.005.

[21] Reynders G, Diriken J, Saelens D. Quality of grey-box models and identified parameters as function of the accuracy of input and observation signals. Energy Build 2014;82:263–74. https://doi.org/10.1016/j.enbuild.2014.07.025.

[22] Andersson JAE, Gillis J, Rawlings GH, J B, Diehl M. CasADi – a software framework for nonlinear optimization and optimal control. Math. Program. Comput. 2019;11(1):1–36. https://doi.org/10.1007/s12532-018-0139-4.

[23] Wächter A, Biegler LT. On the implementation of an interior-point filter line-search algorithm for large-scale nonlinear programming. Math Program 2006;106(1):25–57. https://doi.org/10.1007/s10107-004-0559-y.

[24] Servicepunt Duurzame Energie. Duurzame warmte – de technieken van de warmtetransitie voor gebouwde omgeving. 2019.

[25] Averfalk H, Benakopoulos T, Best I, Dammel F, Engel C, Geyer R, Gudmundsson O, Lygnerud K, Nord N, Oltmanns J, Ponweiser K, Schmidt D, Schrammel H, Ostergaard DS, Svendsen S, Tunzi M, Werner S. Low-temperature district heating implementation guidebook. 2021.